

# Asymptomatic carotid artery stenosis is associated with cerebral hypoperfusion

Amir A. Khan, PhD,<sup>a</sup> Jigar Patel, MD,<sup>b</sup> Sarasijhaa Desikan, MD,<sup>c,d</sup> Matthew Chrencik, BS,<sup>c,d</sup> Janice Martinez-Delcid, BS,<sup>c,d</sup> Brian Caraballo, BS,<sup>c,d</sup> John Yokemick, RVT,<sup>c,d</sup> Vicki L. Gray, PhD,<sup>e</sup> John D. Sorkin, MD, PhD,<sup>f,g</sup> Juan Cebral, PhD,<sup>a</sup> Siddhartha Sikdar, PhD,<sup>a</sup> and Brajesh K. Lal, MD,<sup>c,d</sup> *Fairfax, Va; and Baltimore, Md*

## ABSTRACT

**Objective:** We have shown that almost 50% of patients with asymptomatic carotid stenosis (ACS) will demonstrate cognitive impairment. Recent evidence has suggested that cerebral hypoperfusion is an important cause of cognitive impairment. Carotid stenosis can restrict blood flow to the brain, with consequent cerebral hypoperfusion. In contrast, cross-hemispheric collateral compensation through the Circle of Willis, and cerebrovascular vasodilation can also mitigate the effects of flow restriction. It is, therefore, critical to develop a clinically relevant measure of net brain perfusion in patients with ACS that could help in risk stratification and in determining the appropriate treatment. To determine whether ACS results in cerebral hypoperfusion, we developed a novel approach to quantify interhemispheric cerebral perfusion differences, measured as the time to peak (TTP) and mean transit time (MTT) delays using perfusion-weighted magnetic resonance imaging (PWI) of the whole brain. To evaluate the utility of using clinical duplex ultrasonography (DUS) to infer brain perfusion, we also assessed the relationship between the PWI findings and ultrasound-based peak systolic velocity (PSV).

**Methods:** Structural and PWI of the brain and magnetic resonance angiography of the carotid arteries were performed in 20 patients with  $\geq 70\%$  ACS. DUS provided the PSV, and magnetic resonance angiography provided plaque geometric measures at the stenosis. Volumetric perfusion maps of the entire brain from PWI were analyzed to obtain the mean interhemispheric differences for the TTP and MTT delays. In addition, the proportion of brain volume that demonstrated a delay in TTP and MTT was also measured. These proportions were measured for increasing severity of perfusion delays (0.5, 1.0, and 2.0 seconds). Finally, perfusion asymmetries on PWI were correlated with the PSV and stenosis features on DUS using Pearson's correlation coefficients.

**Results:** Of the 20 patients, 18 had unilateral stenosis (8 right and 10 left) and 2 had bilateral stenoses. The interhemispheric (left–right) TTP delays measured for the whole brain volume identified impaired perfusion in the hemisphere ipsilateral to the stenosis in 16 of the 18 patients. More than 45% of the patients had had ischemia in at least one half of their brain volume, with a TTP delay  $>0.5$  second. The TTP and MTT delays showed strong correlations with PSV. In contrast, the correlations with the percentage of stenosis were weaker. The correlations for the PSV were strongest with the perfusion deficits (TTP and MTT delays) measured for the whole brain using our proposed algorithm ( $r = 0.80$  and  $r = 0.74$ , respectively) rather than when measured on a single magnetic resonance angiography slice as performed in current clinical protocols ( $r = 0.31$  and  $r = 0.58$ , respectively).

**Conclusions:** Interhemispheric TTP and MTT delay measured for the whole brain using PWI has provided a new tool for assessing cerebral perfusion deficits in patients with ACS. Carotid stenosis was associated with a detectable reduction in ipsilateral brain perfusion compared with the opposite hemisphere in  $>80\%$  of patients. The PSV measured at the carotid stenosis using ultrasonography correlated with TTP and MTT delays and might serve as a clinically useful surrogate to brain hypoperfusion in these patients. (*J Vasc Surg* 2021;73:1611–21.)

**Keywords:** Atherosclerosis; Carotid; Cerebral hemodynamics; Perfusion imaging; Stenosis

From the Department of Bioengineering, George Mason University, Fairfax<sup>a</sup>; the Imaging Service, Veterans Affairs Maryland Health Care System, Baltimore<sup>b</sup>; the Department of Vascular Surgery, University of Maryland School of Medicine, Baltimore<sup>c</sup>; the Vascular Service, Veterans Affairs Medical Center, Baltimore<sup>d</sup>; the Department of Physical Therapy and Rehabilitation Science, University of Maryland School of Medicine, Baltimore<sup>e</sup>; the Geriatric Research, Education, and Clinical Center, Baltimore Veterans Affairs Medical Center, Baltimore<sup>f</sup>; and the Claude D. Pepper Older Americans Independence Center, University of Maryland School of Medicine, Baltimore.<sup>g</sup>

The present study was supported by Veterans Affairs Merit Awards (grants RX000995 and CX001621), the National Institutes of Health (grants NS080168, NS097876, and AG000513 to B.K.L. and grants AG028747 and DK072488 to J.D.S.), and the Geriatric Research, Education, and Clinical Center, Baltimore Veterans Affairs Medical Center (to J.D.S.). The funding agencies had no involvement in the study design or collection, analysis, and

interpretation of data. The listed funding agencies were not involved in the decision to submit the report for publication.

Author conflict of interest: none.

Additional material for this article may be found online at [www.jvascsurg.org](http://www.jvascsurg.org).

Correspondence: Brajesh K. Lal, MD, Department of Vascular Surgery, University of Maryland Medical Center, 22 South Greene St, S10B00, Baltimore, MD 21201 (e-mail: [blal@som.umaryland.edu](mailto:blal@som.umaryland.edu)).

The editors and reviewers of this article have no relevant financial relationships to disclose per the JVS policy that requires reviewers to decline review of any manuscript for which they may have a conflict of interest.

0741-5214

Copyright © 2020 by the Society for Vascular Surgery. Published by Elsevier Inc.

<https://doi.org/10.1016/j.jvs.2020.10.063>

Asymptomatic carotid stenosis (ACS) affects ~4% of adults, with an even greater prevalence in the elderly (~12%).<sup>1-3</sup> We recently showed that patients with ACS can exhibit dysfunction in composite and domain-specific cognitive function compared with age- and vascular risk factor-matched controls.<sup>4</sup> The Rotterdam Scan Study found that cerebral hypoperfusion is an important cause of cognitive dysfunction in community dwelling adults.<sup>5,6</sup> Carotid stenosis can restrict the blood flow to the brain and cause cerebral hypoperfusion. However, cross-collateral compensation of flow through the Circle of Willis and additional compensatory intracerebral vasodilation could collectively mitigate the effects of stenosis-induced flow restriction. However, ~50% of these patients will have partial or complete disconnection of their Circle of Willis. Also, intracerebral vasodilation can vary among individuals and could be inadequate in the presence of intracranial atherosclerosis. Therefore, compensation for the flow restriction from a stenosis varies across the population, and the measurement of the stenosis alone is insufficient to assess its true hemodynamic effects on the brain. Therefore, a need exists to develop a direct clinical measure of net brain perfusion in patients with ACS. The conventional selection of ACS patients for revascularization is informed by the findings from the ACAS (asymptomatic carotid atherosclerosis study), which used the percentage of narrowing of the carotid artery as its criterion for intervention, a metric that has increasingly been shown to be unreliable.<sup>7</sup> An assessment of brain perfusion in these patients could provide additional information for risk stratification.

Perfusion-weighted magnetic resonance imaging (PWI) is a readily available minimally invasive modality in which passage of an injected contrast agent can be serially tracked through the cerebrovascular system.<sup>8-10</sup> The resulting PWI data can be processed to obtain measurements of the cerebral blood volume and cerebral blood flow.<sup>10</sup> The first passage of contrast can be quantified in terms of the time to peak flow (TTP), defined as the mean time in seconds to the arrival of the maximum signal after initiation of the perfusion scan, and mean transit time (MTT), defined as the time in seconds required for the contrast agent to pass through the microcirculation.<sup>9</sup> The MTT is computed as the ratio of blood volume to blood flow.<sup>9</sup> The current clinical PWI protocols measure these parameters from one arbitrarily selected image slice at the level of the basal ganglia of each hemisphere.<sup>11</sup> This allows for quantification of differences in the TTP and MTT between the right and left hemispheres from the single image slice. However, these measurements cannot identify any variability in perfusion that might be present in other

locations of the brain and cannot provide a reliable measure of whole brain perfusion. Therefore, an approach that allows for quantification of whole brain perfusion is required.

Doppler ultrasound-based peak systolic velocity (PSV) measurements are conventionally obtained from patients with ACS during the preliminary assessments of the degree of stenosis.<sup>12</sup> However, the relationship of the PSV to brain perfusion has not yet been evaluated. PSV, which is a dynamic measurement, will be influenced by the stenosis and by cross-collateralization through the Circle of Willis. Therefore, assessments of the relationship between the PSV and cerebral perfusion might provide an effective surrogate for brain perfusion that could help make the risk stratification of patients with ACS more clinically convenient.

In the present study, we measured brain perfusion deficits using the conventional evaluation of PWI by analyzing a single two-dimensional image slice at the level of the basal ganglia in patients with ACS. We also measured perfusion deficits using a novel approach that evaluates PWI of the whole brain in three dimensions. We then determined whether ACS was associated with cerebral hypoperfusion by identifying the proportion of patients demonstrating hypoperfusion and by quantifying the proportion of brain volume affected by hypoperfusion. Finally, we evaluated the relationship between the ultrasound-based PSV at the stenosis and brain perfusion deficits. To the best of our knowledge, the present study is the first to investigate the relationship between ACS and PWI-based cerebral perfusion of the whole brain, quantify the hypoperfusion in terms of the proportional brain volume affected, and define the relationship between the PSV and brain perfusion.

## METHODS

**Patients.** A total of 20 consecutive patients with asymptomatic high-grade carotid stenosis ( $\geq 70\%$  diameter reduction) with normal National Institutes of Health stroke scale and modified Rankin scale scores were selected for the present study. The criterion for  $\geq 70\%$  stenosis was determined by the Doppler ultrasound velocity (PSV  $> 230$  cm/s).<sup>12</sup> Demographic information and comorbidities such as coronary artery disease, diabetes mellitus, hypertension, hypercholesterolemia, smoking history, and peripheral arterial occlusive disease were recorded.<sup>13</sup> The University of Maryland School of Medicine Institutional Review Board approved the present study protocol, and all patients provided written informed consent for participation.

**Imaging.** Carotid duplex ultrasound imaging was performed using a linear array transducer (L15) using a clinical ultrasound machine (Ultrasonix SonixTouch, Richmond, British Columbia, Canada). The spectral Doppler waveforms at the proximal, mid, and distal

common and internal carotid arteries were recorded to obtain the velocity measures in both the ipsilateral and the contralateral arteries.<sup>4,14,15</sup> The patients then underwent three-dimensional T1-weighted magnetic resonance imaging (MRI) of the brain, magnetic resonance angiography of the carotid artery, and PWI of the brain after injection of gadolinium (0.1 mmol/kg dose, injected at 5 mL/s).<sup>16,17</sup> The spatial resolution and slice thickness of the PWI acquisition was  $2 \times 2 \times 3.5$  mm. All MRI was performed using a 3T Philips Scanner (Philips Healthcare, Best, Netherlands). Quantitation of cerebral perfusion dynamics was accomplished using IB Neuro (Imaging Biometrics, Elm Grove, Wis), a plug-in application for Horos (Purview, Annapolis, Md).<sup>18,19</sup> As the gadolinium contrast enters the cerebral circulation, it induces susceptibility changes owing to its paramagnetic properties, leading to signal intensity loss captured by PWI. The perfusion sequence is relatively quick (<2 minutes) as the contrast enters and then leaves the brain and does not add any significant additional overhead to a routine MRI examination. The resulting time curves at each voxel were processed to generate maps of the TTP, MTT, relative cerebral blood flow (rCBF), defined as the computed blood flow of a voxel in arbitrary units, and relative cerebral blood volume (rCBV), defined as the computed volume of a voxel in arbitrary units (saved in DICOM [Digital Imaging and Communications in Medicine] format) for each slice of the PWI (Supplementary Fig, online only).

**Single slice analysis of perfusion at the basal ganglia level.** A board-certified neuroradiologist identified the axial slice of the PWI study at the level of the basal ganglia and outlined both cortical hemispheres (ie, excluding the ventricles). The interhemispheric perfusion differences between the two cerebral hemispheres for each of the four perfusion measures (TTP, MTT, rCBF, rCBV) were computed as the difference in the mean values of the perfusion parameters between the left and right hemispheres visible on the image slice.

**Whole brain analysis.** The T1-weighted structural brain volumes were normalized to the standard Montreal Neurological Institute brain atlas using FreeSurfer software (General Hospital Corp, Boston, Mass).<sup>20-23</sup> The resulting volumes had the spatial resolution of  $2 \times 2 \times 2$  mm and allowed for a standardized comparison across patients. The raw perfusion maps were then co-registered with the structural MRI scans to automatically generate outlines for the left and right hemispheres in the entire brain across all slices using statistical parametric mapping.<sup>24,25</sup> This automation removed any operator bias for outlining the hemispheres. For each subject, the mean perfusion value for TTP, MTT, rCBF, and rCBV was computed for each hemisphere for the entire brain across all slices. Histograms for the left and right

hemispheres were analyzed to remove any outliers. The interhemispheric perfusion differences were then computed for the mean value of each parameter (TTP, MTT, rCBF, rCBV). The interhemispheric time delays were typically on the order of tenths of a second to several seconds (depending on the nature of the disease).

**Proportional brain volume analysis.** Of the four measures of perfusion, TTP and MTT are the most sensitive identifiers of early perfusion deficits, because they incorporate the timing information of the contrast agent as it washes through different regions of brain.<sup>26,27</sup> To assess the volume of the brain affected by hypoperfusion and the severity of hypoperfusion in different regions of the brain, we quantified the TTP and MTT delays between the left and right hemispheres at four temporal hypoperfusion thresholds: >0.5 second, >1 second, and >2 seconds. We devised a method that allowed us to compute the voxel-level interhemispheric delays between the left and right hemispheres. We quantified the passage of contrast through one voxel in one hemisphere and compared it with the corresponding voxel in the opposite hemisphere. The TTP and MTT maps for each subject were co-registered to their T1-weighted structural images and normalized to the symmetric Montreal Neurological Institute template.<sup>28</sup> To allow for a voxel-level analysis, the maps were smoothed using a Gaussian blurring filter to remove the influence of spurious voxels that were generated during the normalization process. These processed maps were then used to compute the proportion of hemispheric brain volume corresponding to TTP and MTT delays of >0.5 second, >1 second, and >2 seconds in flow to one side vs the other side of the brain. Details of the method used to determine temporal hypoperfusion are presented in the Supplementary Fig (online only).

**Statistical analysis.** The interhemispheric TTP and MTT delays were computed in seconds and the rCBV and rCBF differences in arbitrary units. The degree of stenosis was characterized in one and two dimensions: the minimum luminal diameter at the stenosis in millimeters, minimum luminal cross-sectional area at the stenosis in square millimeters, maximum percentage of stenosis by diameter (MSD), and maximum percentage of stenosis by area (MSA). The MSD and MSA were computed using the distal internal carotid artery with parallel walls as the denominator (NASCET [North American Symptomatic Carotid Endarterectomy Trial Collaborators] criteria).<sup>29</sup> Scatter plots were used to visualize the relationship between the PSV at the stenosis and the interhemispheric perfusion differences. The single slice and whole brain analyses were represented on the same figures. The relationship between the interhemispheric perfusion differences and stenosis measurements (PSV, minimum diameter, area at stenosis, MSD, and MSA) are expressed

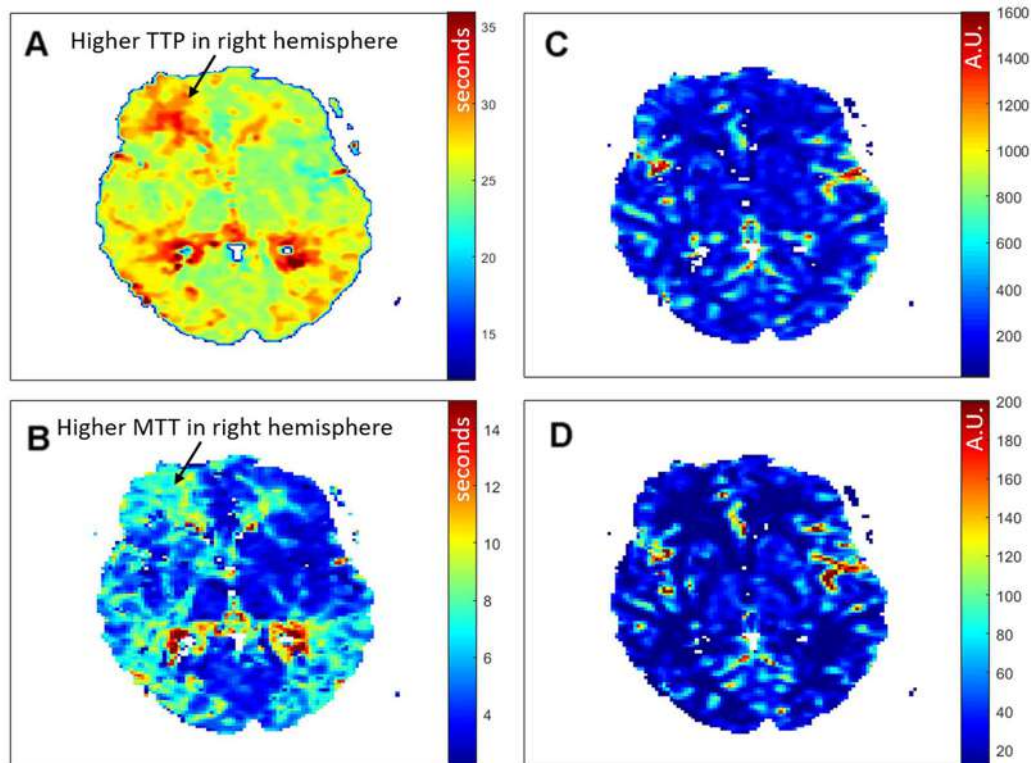


**Fig 1.** Raw perfusion maps at the level of basal ganglia for a sample patient with a right-sided stenosis: time to peak (*TTP*; **A**), mean transit time (*MTT*; **B**), relative cerebral blood volume (*rCBV*; **C**), and relative cerebral blood flow (*rCBF*; **D**). Interhemispheric perfusion differences are visible, especially for *TTP* (arrow in **A**) and *MTT* maps. No difference was found in perfusion between hemispheres when the color in any given part of the brain was the same in the two hemispheres. *Blue* and *red* represent the lowest and highest values in each scan, respectively. The ventricles in each hemisphere were excluded from the analysis. *A.U.*, Arbitrary units.

using Pearson's correlation coefficients. Statistical analysis was performed using MATLAB, version R2016b (MathWorks Inc, Natick, Mass). A two-tailed  $P < .05$  was considered to indicate statistical significance.

## RESULTS

**Patient characteristics.** The mean age of the patients was  $67 \pm 11$  years and 84% were men (Supplementary Table I, online only). As would be expected, the risk factors for vascular disease were very common in the patients. Of the 20 patients, 18 had unilateral and 2 had bilateral stenoses. The patients had a mean  $\pm$  standard deviation PSV at the stenosis of  $436 \pm 141$  cm/s on the ipsilateral side and  $119 \pm 72$  cm/s on the contralateral side.

**Interhemispheric perfusion differences.** The raw perfusion maps of a subject with a right-sided stenosis in a single slice at the level of the basal ganglia are presented in Fig 1. A clear asymmetry between the left and the right hemispheres was manifested in this patient, which was especially evident in the *TTP* and *MTT* maps (Fig 1, A and B, arrow).

The differences between hemispheres for the four perfusion parameters are shown in Fig 2. The single slice

and whole brain analyses are presented adjacent to each other. Perfusion differences were computed from left to right. Therefore, a negative *TTP* value indicates that the time taken for the contrast agent to pass through the right hemisphere was longer than the time required for the left. A *TTP* delay was identified on the side of the stenosis in 15 of the 18 patients (83%) with a unilateral stenosis on single slice analysis. Both of the patients with bilateral stenosis had experienced a *TTP* delay on the right side. The *TTP* for the whole brain was delayed in 16 of the 18 patients (89%) with unilateral stenosis, with 1 of the 2 patients with bilateral stenosis exhibiting no delay and one, a right-sided delay. An *MTT* delay was observed in 16 of the 18 patients (89%) on both single slice and whole brain analysis. The *rCBF* was reduced on the stenosis side in 16 (89%) and 15 (83%) of the 18 patients on single and whole brain analysis, respectively. The *rCBV* was reduced in 7 of the 18 patients (39%) on the stenosed side using both single and whole brain analysis. The interhemispheric asymmetries across the entire cohort are summarized in Supplementary Table II (online only).

The percentage of hypoperfused brain volume is shown in Fig 3. As expected, the results varied, depending on the threshold used to define hypoperfusion. The results are



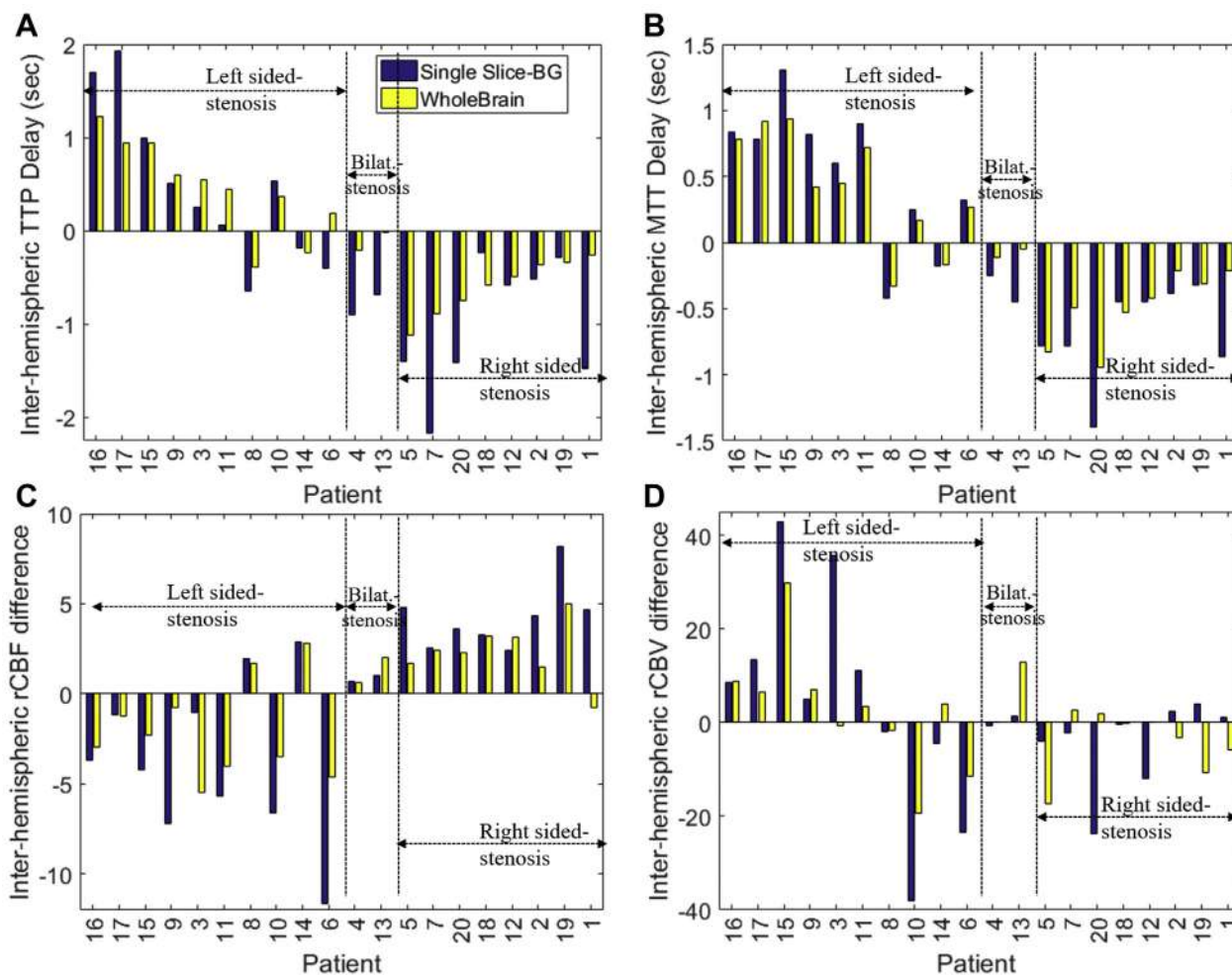


**Fig 2.** Interhemispheric (left–right) differences in perfusion parameters at the level of the basal ganglia and whole brain: time to peak (*TTP*; **A**), mean transit time (*MTT*; **B**), relative cerebral blood flow (*rCBF*; **C**), and relative cerebral blood volume (*rCBV*; **D**). Negative values indicate increased perfusion deficits in the right hemisphere because the differences were computed by subtracting the right hemisphere values from those of the left. Laterality is indicated by the sign of the parameter, and the magnitude quantifies the extent of interhemispheric dissimilarity. The patients were arranged by stenosis laterality (left, bilateral, right) and decreasing whole brain *TTP* differences for all four parameters.

presented for increasing thresholds ( $>0.5$  second,  $>1$  second, and  $>2$  seconds) of perfusion delays for *TTP* and *MTT*. A total of nine patients (45%) had had  $\geq 50\%$  of their brain hypoperfused when hypoperfusion was defined as a *TTP* delay  $>0.5$  second. The number was slightly lower when the *MTT* delay was measured at a threshold of  $>0.5$  second at eight patients (40%). When the *TTP* delay threshold was  $>1$  second, three patients (15%) demonstrated hypoperfusion in  $>50\%$  of their brain at that severity and seven (35%) demonstrated hypoperfusion in  $\geq 35\%$  of their brain volume. With a threshold of a  $>2$ -second delay for either *TTP* or *MTT*, two patients had had  $\geq 35\%$  of the brain volume ischemic. Therefore, when the temporal threshold to define hypoperfusion was set at a sensitive level of  $>0.5$  second,

80% of the patients had had hypoperfusion to  $\geq 35\%$  of their brain and 45% had had hypoperfusion to  $\geq 50\%$  of their brain.

The influence of cross-collateralization through the Circle of Willis on the cerebral perfusion is depicted in Fig 4. The perfusion metrics for the 14 patients with a defect in the anterior cerebral circulation (eg, hypoplastic, aplastic, or atherosclerotic segment) was compared with the 6 patients with a completely normal Circle of Willis. The timing parameters, *TTP* delay (Fig 4, A) and *MTT* delay (Fig 4, B), were greater in the presence of an incomplete Circle of Willis compared with an intact one. Statistically significant differences were observed in the *TTP* delay for the whole brain ( $P = .02$ ) and the *MTT* delay for both the whole brain ( $P = .03$ ) and the single slice ( $P = .003$ ) analyses.

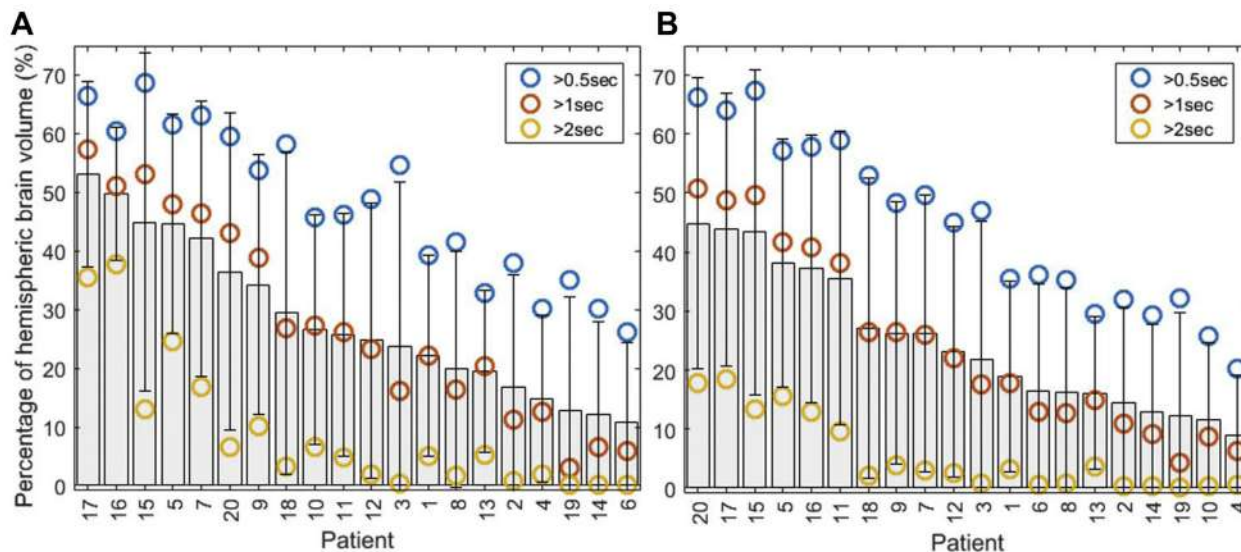


**Fig 3.** Proportion of ipsilateral brain volume with hypoperfusion, when the hypoperfusion threshold was set at a delay of >0.5 second, >1 second, and >2 seconds relative to the contralateral hemisphere using voxel-level analysis for time to peak (TTP; **A**) and mean transit time (MTT; **B**). The threshold of >0.5, 1, and 2-second counted all voxels at which the TTP or MTT was greater than 0.5, 1, or 2 seconds, with the proportion determined by the corresponding hemispheric brain volume. The mean percentage for the three thresholds (gray bars) and standard deviation (error bars) are also presented for each patient. Patients were presented in decreasing order of the mean percentages.

The relationship of the PSV measured at the stenosis using ultrasonography and the measures of interhemispheric perfusion differences using Pearson's correlation coefficient are illustrated in Fig 5 and the Table ( $P < .05$ ). A strong correlation was observed between the PSV and TTP delay for the whole brain ( $r = 0.8$ ), which was also observed between the PSV and MTT delay ( $r = 0.78$ ). The single slice analysis did not depict a clear trend for TTP ( $r = 0.31$ ). However, the MTT performed slightly better against the PSV ( $r = 0.58$ ). The rCBF ( $r = 0.23$  for single slice;  $r = 0.35$  for whole brain) and rCBV ( $r = 0.31$  for single slice;  $r = 0.27$  for whole brain) showed weaker, although correctly directed, trends with the PSV. The minimum diameter at stenosis demonstrated negative correlations with the TTP and MTT measured for the whole brain, albeit weaker than the PSV. Similar trends were observed when other stenosis measurements were correlated with the whole brain perfusion measures. The end-diastolic velocities and the ratios of PSVs in the internal and common carotid arteries showed results consistent with the PSVs and correlated with the brain perfusion measures, especially the TTP delay. The correlation coefficients are presented in detail in the Table. Finally, the PSV for the patients with defects in their anterior Circle of Willis circulation (hypoplastic/aplastic and atherosclerotic segments) was greater ( $461.07 \pm 160.11$  cm/s) than that in the group with no defects ( $378.67 \pm 61.31$  cm/s).

## DISCUSSION

We have described a method that computes the interhemispheric cerebral perfusion differences for the whole brain using clinically acquired PWI. A large proportion of patients with neurologically asymptomatic carotid artery stenosis demonstrated cerebral hypoperfusion on PWI. The four perfusion parameters measured (ie, TTP, MTT, rCBF, rCBV) identified impaired cerebral perfusion in 88% of patients with asymptomatic high-grade ( $\geq 70\%$ ) carotid stenosis. Most patients demonstrated a TTP delay of >0.5 second in at least one half of the affected cerebral hemisphere and a TTP delay of >1.0 second in  $\geq 35\%$  of the affected hemisphere. The PSVs measured on clinical duplex ultrasonography correlated with the MRI measures of cerebral hypoperfusion, especially with respect to the TTP ( $r = 0.80$ ) and MTT ( $r = 0.78$ ).

Our computer circuit modeling had previously predicted that narrowing of the carotid artery would result in a pressure gradient across the stenosis that could be compensated for by collateral circulation from the opposite hemisphere via the Circle of Willis.<sup>30</sup> The Circle of Willis is, however, known to be incomplete (with segments that can be hypoplastic, aplastic, or diseased) in a large proportion of the population.<sup>31</sup> Therefore, we anticipated that many patients with carotid stenosis could experience a decrease in pressure across their stenosis that remained undercompensated through the collateral circuits, thereby rendering the brain hypoperfused. The results of the present study have provided confirmation

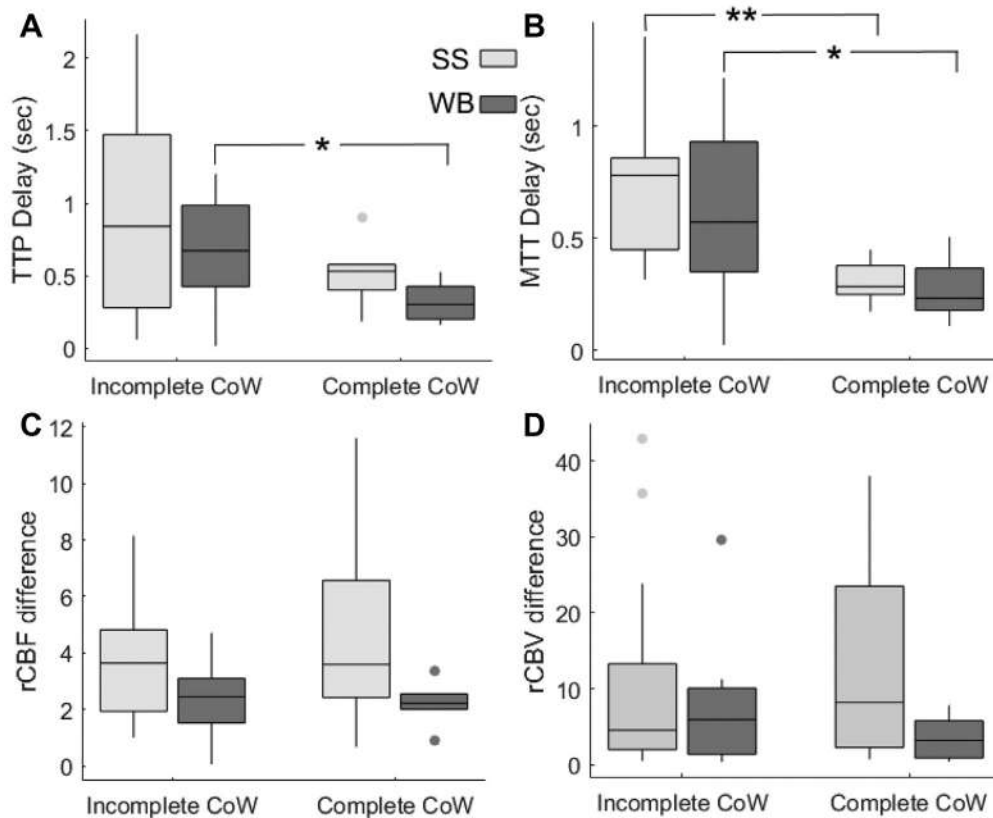


**Fig 4.** Interhemispheric perfusion differences (absolute values) as a function of collateralization through the Circle of Willis (CoW) for whole brain (WB) and single slice (SS) analysis. Time to peak (TTP; **A**), mean transit time (MTT; **B**), relative cerebral blood flow (rCBF; **C**), and relative cerebral blood volume (rCBV; **D**). \* $P < .05$ ; \*\* $P < .005$ .

of brain hypoperfusion in a large proportion of patients with high-grade ACS, especially in the absence of effective collateralization through the Circle of Willis (Figs 3 and 4).

PWI is a clinically, reliable, noninvasive tool for quantifying interhemispheric cerebral perfusion differences in patients with ACS. Previous studies have assessed several PWI parameters in selected brain image slices in a mix of symptomatic and asymptomatic patients with ACS.<sup>32</sup> The present study focused solely on asymptomatic patients and extended the scope of the analysis to the whole brain. The TTP and MTT parameters appeared to be the most sensitive to perfusion differences because these two parameters directly track the traversal of contrast as it passes from the cervical to the cerebral vascular circuit. The rCBV and rCBF are not expected to be as sensitive to the stenosis as the two time-related parameters.<sup>26</sup> Conventionally, clinical radiologists have assessed these maps in a single image slice subjectively selected at the level of the basal ganglia. We have developed an efficient method for analyzing imaging data from the entire brain volume that is more representative of the perfusion status of the entire brain. The results for TTP and MTT obtained using this approach identified more patients (88%) with interhemispheric perfusion

deficits than were obtained by comparing perfusion at a single arbitrary slice at the basal ganglia level as most commonly used in current clinical practice.<sup>11</sup>

Several chronic diseases are known to be associated with cerebral hypoperfusion, and these, in turn, have been correlated with cognitive and mobility dysfunction and progression to dementia.<sup>33</sup> Cerebral hypoperfusion from intracranial vasculopathy due to diabetes, hypertension, and sleep apnea<sup>34,35</sup> and cerebral hypoperfusion from cardiac failure both result in cognitive dysfunction.<sup>36,37</sup> The existence of clinical comorbidities (eg, diabetes, coronary artery disease, hypertension, smoking, hyperlipidemia) did not influence the perfusion metrics for our cohort, with no significant differences found on the *t* tests between the groups with and without these comorbidities (data not shown). Similarly, balloon occlusion or clamping of the carotid artery leads to attentional deficits proportionate to the degree of reduction in blood flow to the brain.<sup>38,39</sup> In older individuals and, especially, in older patients with diabetes, impaired cerebral perfusion during exertional stress is also associated with reduced gait speed and falls.<sup>40,41</sup> We recently reported that overall cognitive function and the domain-specific functions of fine motor and processing speed, learning and memory, and executive function were

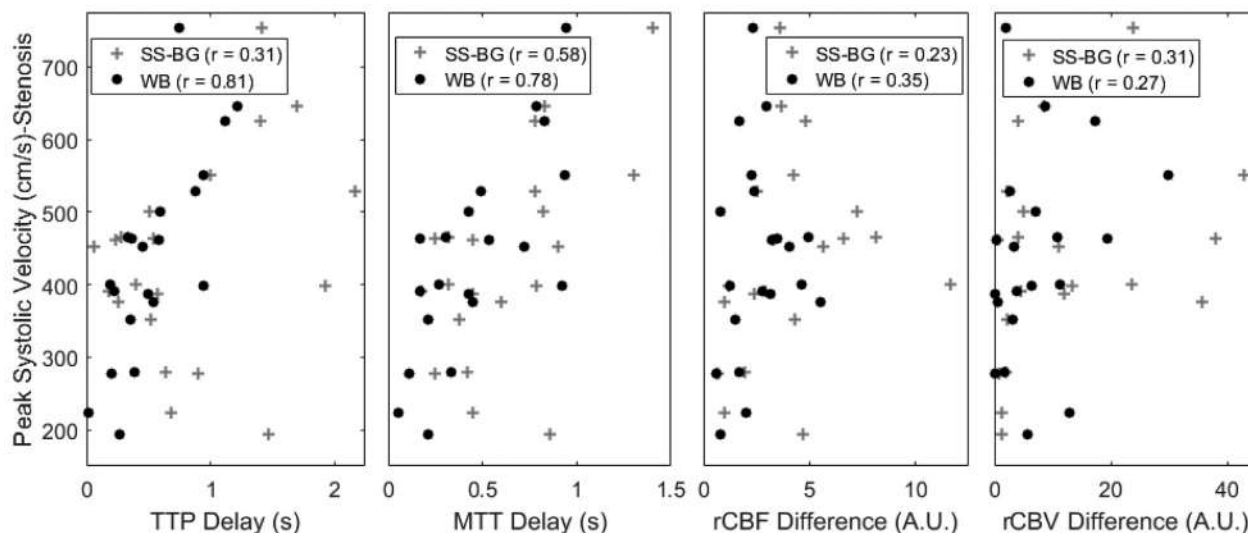


**Fig 5.** The in vivo peak systolic velocity (PSV) measured at stenosis using Doppler ultrasonography as a function of the magnitude of interhemispheric differences in perfusion parameters. A.U., Arbitrary units; MTT, mean transit time; rCBF, relative cerebral blood flow; rCBV, relative cerebral blood volume; SS-BG, single-slice at basal ganglia; TTP, time to peak; WB, whole brain.

**Table.** Correlation coefficients between perfusion parameters and stenosis measurements<sup>a</sup>

	PSV		EDV		ICA/CCA		MDS		MDA		MSD		MSA	
	SS-BG	WB	SS-BG	WB	SS-BG	WB	SS-BG	WB	SS-BG	WB	SS-BG	WB	SS-BG	WB
TTP	0.31	<b>0.81</b>	0.30	0.65	0.34	0.78	-0.17	-0.55	-0.16	-0.44	0.22	0.55	0.15	0.44
MTT	0.58	<b>0.78</b>	0.50	0.60	0.46	0.63	-0.56	-0.53	-0.55	-0.47	0.42	0.48	0.38	0.42
rCBF	0.23	0.35	0.32	0.39	0.32	0.19	-0.27	-0.29	-0.28	-0.19	0.28	0.25	0.30	0.18
rCBV	0.31	0.27	0.32	0.20	0.32	0.18	-0.36	-0.47	-0.42	-0.41	0.32	0.46	0.37	0.38

EDV, End-diastolic velocity; ICA/CCA, internal carotid artery to common carotid artery velocity ratio; MDA, minimum area at stenosis; MDS, minimum diameter at stenosis; MSA, maximum stenosis by area; MSD, maximum stenosis by diameter; MTT, mean transit time; PSV, peak systolic velocity; rCBF, relative cerebral blood flow; rCBV, relative cerebral blood volume; SS-BG, single-slice at basal ganglia; TTP, time to peak; WB, whole brain. Boldface values represent highest correlations.

<sup>a</sup>All correlations reported were significant at  $P < .05$ .

impaired in patients ACS compared with age- and vascular risk factor-matched controls.<sup>42</sup> These impairments were not related to plaque disruption and could be related to cerebral hemodynamics. Additional studies have also reported that ACS is associated with reduced global cognition (MMSE [mini-mental state examination]<sup>43</sup> and MOCA [Montreal cognitive assessment]<sup>44</sup>), reduced scores for tests of mental speed, learning, visuospatial abilities, verbal processing, and reasoning<sup>45,46</sup> and for executive function<sup>6</sup> compared with healthy controls. Mobility impairment coexists with cognitive dysfunction in many older adults.<sup>47-53</sup> In addition, mobility dysfunction shares most of the vascular risk factors that also affect cognition.<sup>54-59</sup> We have recently reported that patients with ACS have declining gait speed and balance function.<sup>60</sup> Our findings of cerebral hypoperfusion resulting from flow restriction in patients with ACS in the

present study can explain the cognitive and mobility impairments identified in these patients.

The true contribution of carotid stenosis to cerebral hypoperfusion can only be determined after accounting for both the pressure decrease across the stenosis and the pressure generated from cross-collateralization.<sup>30,61-64</sup> Thus, it can be anticipated that the net PSV measured at the stenosis would be affected by both the degree of narrowing at the stenosis and the extent of cross-collateral flow. Our computer circuit model predicted that a 70% carotid stenosis in the presence of a completely disconnected Circle of Willis would result in a higher PSV compared with a 70% stenosis in the presence of an intact Circle of Willis.<sup>30</sup> In the present study, we have confirmed these findings in actual patients with carotid stenosis. The PSV for patients with defects in their anterior Circle of Willis circulation (hypoplastic/



aplastic and atherosclerotic segments) was higher ( $461.07 \pm 160.11$  cm/s) compared with that of the group with no defects ( $378.67 \pm 61.31$  cm/s). Therefore, in the present study, we hypothesized that severely elevated PSVs could be a marker for cerebral hypoperfusion. Our results have demonstrated that cerebral hypoperfusion measured by quantitative volumetric PWI is strongly related to the in vivo velocity measurements at the stenosis. These results suggest that, in addition to defining the degree of stenosis, the PSV in patients with ACS is a potentially useful marker of cerebral perfusion.

Although we found a strong relationship between the in vivo PSV measurements and perfusion parameters for the whole brain (TTP and MTT), an appropriate threshold for the PSV that would indicate significant cerebral hypoperfusion requires a larger patient cohort and is being pursued in an ongoing study. Although we found clear evidence for cerebral hypoperfusion in neurologically asymptomatic patients, in contrast to stroke patients, the differences between the ipsilateral and contralateral hemispheres were more subtle in this asymptomatic population. Very limited data are available to suggest clinically significant thresholds for brain hypoperfusion in general, with none reported for the ACS population. This is the direct result of (1) the lack of a sensitive protocol to objectively quantify brain perfusion, and (2) the lack of sensitive tools to measure the clinical consequences of the hypoperfusion beyond simple neurologic sensory and motor testing. In the present report, we have offered a solution that quantifies brain perfusion. In previous reports, we provided evidence for subtle, yet clinically important, cognitive and mobility impairments in these patients. A larger study is ongoing to test how these perfusion delays correlate with the cognitive and mobility function assessment scores. This could potentially lead to the identification of a subpopulation of ACS patients who might benefit from more aggressive treatment.

## CONCLUSIONS

Cerebral hypoperfusion is known to be associated with cognitive and mobility dysfunction in several chronic disease states. We have described a clinically applicable approach to quantifying cerebral perfusion deficits for the whole brain using PWI. We found that a large proportion of patients with neurologically asymptomatic high-grade carotid stenosis demonstrated detectable cerebral hypoperfusion. The in vivo ultrasound-based PSV at the stenosis correlated with the interhemispheric TTP delay and MTT delay derived from the PWI and might serve as a surrogate measure of cerebral perfusion status. Knowledge of cerebral hypoperfusion might assist in the risk stratification of patients with ACS.

## AUTHOR CONTRIBUTIONS

Conception and design: AK, JP, SD, MC, VG, JC, SS, BL  
Analysis and interpretation: AK, JP, MC, JMD, BC, JS, SS, BL  
Data collection: JP, JY, BL  
Writing the article: AK, JP, BL

Critical revision of the article: AK, JP, SD, MC, JMD, BC, JY, VG, JS, JC, SS, BL

Final approval of the article: AK, JP, SD, MC, JMD, BC, JY, VG, JS, JC, SS, BL

Statistical analysis: AK, JS

Obtained funding: JS, BL

Overall responsibility: BL

## REFERENCES

1. European Carotid Surgery Trialists Collaborative Group. Risk of stroke in the distribution of an asymptomatic carotid artery. *Lancet* 1995;345:209-12.
2. Mineva PP, Manchev IC, Hadjiev DI. Prevalence and outcome of asymptomatic carotid stenosis: a population-based ultrasonographic study. *Eur J Neurol* 2002;9:383-8.
3. de Weerd M, Greving JP, de Jong AW, Buskens E, Bots ML. Prevalence of asymptomatic carotid artery stenosis according to age and sex. *Stroke* 2009;40:1105-13.
4. Lal BK, Dux MC, Sikdar S, Goldstein C, Khan AA, Yokemick J, et al. Asymptomatic carotid stenosis is associated with cognitive impairment. *J Vasc Surg* 2017;66:1083-92.
5. Silvestrini M, Vernieri F, Pasqualetti P, Mattei M, Passarelli F, Troisi E, et al. Impaired cerebral vasoreactivity and risk of stroke in patients with asymptomatic carotid artery stenosis. *JAMA* 2000;283:2122-7.
6. Balestrini S, Peruzzi C, Altamura C, Vernieri F, Luzzi S, Bartolini M, et al. Severe carotid stenosis and impaired cerebral hemodynamics can influence cognitive deterioration. *Neurology* 2013;80:2145-50.
7. Brott TC, Halperin JL, Abbara S, Bacharach JM, Barr JD, Bush RL, et al. 2011 ASA/ACCF/AHA/AANN/AANS/ACR/ASNR/CNS/SAIP/SCAI/SIR/SNIS/SVM/SVS guideline on the management of patients with extracranial carotid and vertebral artery disease: a report of the American College of Cardiology Foundation/American Heart Association Task Force on practice guidelines, and the American Stroke Association, American Association of Neuroscience Nurses, American Association of Neurological Surgeons, American College of Radiology, American Society of Neuroradiology, Congress of Neurological Surgeons, Society of Atherosclerosis Imaging and Prevention, Society for Cardiovascular Angiography and Interventions, Society of Interventional Radiology, Society of Neurointerventional Surgery, Society for Vascular Medicine, and Society for Vascular Surgery developed in collaboration with the American Academy of Neurology and Society of Cardiovascular Computed Tomography. *J Am Coll Cardiol* 2011;57:e16-94.
8. Lev MH, Rosen BR. Clinical applications of intracranial perfusion MR imaging. *Neuroimaging Clin North Am* 1999;9:309-31.
9. Petrella JR, Provenzale JM. MR perfusion imaging of the brain: techniques and applications. *AJR Am J Roentgenol* 2000;175:207-19.
10. Cha S. Perfusion MR imaging: basic principles and clinical applications. *Magn Reson Imaging Clin* 2003;11:403-13.
11. Derdeyn CP, Grubb RL, Powers WJ. Cerebral hemodynamic impairment: methods of measurement and association with stroke risk. *Neurology* 1999;53:251-9.
12. Grant EG, Benson CB, Moneta GL, Alexandrov AV, Baker JD, Bluth EI, et al. Carotid artery stenosis: gray-scale and Doppler US diagnosis—Society of Radiologists in Ultrasound Consensus Conference 1. *Radiology* 2003;229:340-6.
13. Romero JR, Beiser A, Seshadri S, Benjamin EJ, Polak JF, Vasan RS, et al. Carotid artery atherosclerosis, MRI indices of brain ischemia, aging, and cognitive impairment. *Stroke* 2009;40:1590-6.
14. Intersocietal Accreditation Commission. IAC Standards and Guidelines for Vascular Testing Accreditation 2020. Available at: <https://www.intersocietal.org/vascular/standards/IACVascularTestingStandards2020.pdf>. Accessed November 30, 2020.
15. Khan AA, Koudelka C, Goldstein C, Zhao L, Yokemick J, Dux M, et al. Semiautomatic quantification of carotid plaque volume with three-dimensional ultrasound imaging. *J Vasc Surg* 2017;65:1407-17.
16. Tombach B, Benner T, Reimer P, Schuierer G, Fallenberg E-M, Geens V, et al. Do highly concentrated gadolinium chelates improve MR brain perfusion imaging? Intraindividually controlled randomized crossover concentration comparison study of 0.5 versus 1.0 mol/L gadobutrol. *Radiology* 2003;226:880-8.

17. Essig M, Lodemann K-P, Le-Huu M, Brüning R, Kirchin M, Reith W. Intraindividual comparison of gadobenate dimeglumine and gadobutrol for cerebral magnetic resonance perfusion imaging at 1.5 T. *Invest Radiol* 2006;41:256-63.
18. Kennan RP, Jäger HR. T2- and T2\*-w DCE-MRI: blood perfusion and volume estimation using bolus tracking. In: Tofts P, editor. *Quantitative MRI of the Brain: Measuring Changes Caused by Disease*. Hoboken, NJ: Wiley; 2003. p. 365-412.
19. Covarrubias DJ, Rosen BR, Lev MH. Dynamic magnetic resonance perfusion imaging of brain tumors. *Oncologist* 2004;9:528-37.
20. Mazziotta J, Toga A, Evans A, Fox P, Lancaster J, Zilles K, et al. A probabilistic atlas and reference system for the human brain: International Consortium for Brain Mapping (ICBM). *Philos Trans R Soc Lond B Biol Sci* 2001;356:1293-322.
21. Dale AM, Fischl B, Sereno MI. Cortical surface-based analysis: I. Segmentation and surface reconstruction. *Neuroimage* 1999;9:179-94.
22. Fischl B, Salat DH, Busa E, Albert M, Dieterich M, Haselgrove C, et al. Whole brain segmentation: automated labeling of neuroanatomical structures in the human brain. *Neuron* 2002;33:341-55.
23. Desikan RS, Ségonne F, Fischl B, Quinn BT, Dickerson BC, Blacker D, et al. An automated labeling system for subdividing the human cerebral cortex on MRI scans into gyral based regions of interest. *Neuroimage* 2006;31:968-80.
24. Friston KJ, Ashburner J, Frith CD, Poline J-B, Heather JD, Frackowiak RS. Spatial registration and normalization of images. *Hum Brain Mapp* 1995;3:165-89.
25. Penny WD, Friston KJ, Ashburner JT, Kiebel SJ, Nichols TE, editors. *Statistical Parametric Mapping: The Analysis of Functional Brain Images*. Cambridge, MA: Academic Press; 2011.
26. Teng MMH, Cheng H-C, Kao Y-H, Hsu L-C, Yeh T-C, Hung C-S, et al. MR perfusion studies of brain for patients with unilateral carotid stenosis or occlusion: evaluation of maps of "time to peak" and "percentage of baseline at peak. *J Comput Assist Tomogr* 2001;25:121-5.
27. Piñero P, González A, Moniche F, Martínez E, Cayuela A, González-Marcos J-R, et al. Progressive changes in cerebral perfusion after carotid stenting: a dynamic susceptibility contrast perfusion weighted imaging study. *J Neurointerventional Surg* 2014;6:527-32.
28. Fonov VS, Evans AC, McKinstry RC, Almlri CR, Collins DL. Unbiased nonlinear average age-appropriate brain templates from birth to adulthood. *NeuroImage* 2011;54:313-27.
29. North American Symptomatic Carotid Endarterectomy Trial Collaborators, Barnett HJM, Taylor DW, Haynes RB, Sackett DL, Peerless SJ, et al. Beneficial effect of carotid endarterectomy in symptomatic patients with high-grade carotid stenosis. *N Engl J Med* 1991;325:445-53.
30. Lal BK, Beach KW, Sumner DS. Intracranial collateralization determines hemodynamic forces for carotid plaque disruption. *J Vasc Surg* 2011;54:1461-71.
31. Alpers B, Berry R, Paddison R. Anatomical studies of the circle of Willis in normal brain. *AMA Arch Neurol Psychiatry* 1959;81:409-18.
32. Kajimoto K, Moriwaki H, Yamada N, Hayashida K, Kobayashi J, Miyashita K, et al. Cerebral hemodynamic evaluation using perfusion-weighted magnetic resonance imaging: comparison with positron emission tomography values in chronic occlusive carotid disease. *Stroke* 2003;34:1662-6.
33. Wolters FJ, Zonneveld HI, Hofman A, van der Lugt A, Koudstaal PJ, Vernooij MW, et al. Cerebral perfusion and the risk of dementia: a population-based study. *Circulation* 2017;136:719-28.
34. Ruitenberg A, den Heijer T, Bakker SL, van Swieten JC, Koudstaal PJ, Hofman A, et al. Cerebral hypoperfusion and clinical onset of dementia: the Rotterdam study. *Ann Neurol* 2005;57:789-94.
35. Daulatzai MA. Cerebral hypoperfusion and glucose hypometabolism: key pathophysiological modulators promote neurodegeneration, cognitive impairment, and Alzheimer's disease. *J Neurosci Res* 2017;95:943-72.
36. Zuccalà G, Cattel C, Manes-Gravina E, Di Niro MG, Cocchi A, Bernabei R. Left ventricular dysfunction: a clue to cognitive impairment in older patients with heart failure. *J Neurol Neurosurg Psychiatry* 1997;63:509-12.
37. Pullicino PM, Hart J. Cognitive impairment in congestive heart failure?: embolism vs hypoperfusion. *Neurology* 2001;57:1945-6.
38. Marshall RS, Lazar RM, Mohr JP, Pile-Spellman J, Hacein-Bey L, Duong DH, et al. Higher cerebral function and hemispheric blood flow during awake carotid artery balloon test occlusions. *J Neurol Neurosurg Psychiatry* 1999;66:734-8.
39. Marshall RS. The functional relevance of cerebral hemodynamics: why blood flow matters to the injured and recovering brain. *Curr Opin Neurol* 2004;17:705-9.
40. Sorond FA, Galica A, Serrador JM, Kiely DK, Iloputaife I, Cupples LA, et al. Cerebrovascular hemodynamics, gait, and falls in an elderly population: MOBILIZE Boston Study. *Neurology* 2010;74:1627-33.
41. Jor'dan AJ, Manor B, Novak V. Slow gait speed—an indicator of lower cerebral vasoreactivity in type 2 diabetes mellitus. *Front Aging Neurosci* 2014;6:1-9.
42. Lal BK, Dux MC, Sikdar S, Goldstein C, Khan AA, Yokemick J, et al. Asymptomatic carotid stenosis is associated with cognitive impairment. *J Vasc Surg* 2017;66:1083-92.
43. Johnston SC, O'Meara ES, Manolio TA, Lefkowitz D, O'Leary DH, Goldstein S, et al. Cognitive impairment and decline are associated with carotid artery disease in patients without clinically evident cerebrovascular disease. *Ann Intern Med* 2004;140:237-47.
44. Martinic-Popovic I, Lovrencic-Huzjan A, Demarin V. Assessment of subtle cognitive impairment in stroke-free patients with carotid disease. *Acta Clin Croat* 2009;48:231-40.
45. Benke T, Neussl D, Aichner F. Neuropsychological deficits in asymptomatic carotid artery stenosis. *Acta Neurol Scand* 1991;83:378-81.
46. Mathiesen EB, Waterloo K, Joakimsen O, Bakke SJ, Jacobsen EA, Bonna KH. Reduced neuropsychological test performance in asymptomatic carotid stenosis: the Tromso study. *Neurology* 2004;62:695-701.
47. Demnitz N, Esser P, Dawes H, Valkanova V, Johansen-Berg H, Ebmeier KP, et al. A systematic review and meta-analysis of cross-sectional studies examining the relationship between mobility and cognition in healthy older adults. *Gait Posture* 2016;50:164-74.
48. Verghese J, Wang C, Lipton RB, Holtzer R. Motoric cognitive risk syndrome and the risk of dementia. *J Gerontol Ser Biol Sci Med Sci* 2013;68:412-8.
49. Hausdorff JM, Yogev G, Springer S, Simon ES, Giladi N. Walking is more like catching than tapping: gait in the elderly as a complex cognitive task. *Exp Brain Res* 2005;164:541-8.
50. Holtzer R, Verghese J, Xue X, Lipton RB. Cognitive processes related to gait velocity: results from the Einstein aging study. *Neuropsychology* 2006;20:215-23.
51. Beauchet O, Allali G, Anweiler C, Verghese J. Association of motoric cognitive risk syndrome with brain volumes: results from the GAIT study. *J Gerontol Ser Biol Sci Med Sci* 2016;71:1081-8.
52. Quan M, Xun P, Chen C, Wen J, Wang Y, Wang R, et al. Walking pace and the risk of cognitive decline and dementia in elderly populations: a meta-analysis of prospective cohort studies. *J Gerontol A Biol Sci Med Sci* 2017;72:266-70.
53. Studenski S. Utility of brief cognitive and physical assessments in clinical care. *J Gerontol Ser Biol Sci Med Sci* 2017;72:59-60.
54. Welmer AK, Angleman S, Rydwick E, Fratiglioni L, Qiu C. Association of cardiovascular burden with mobility limitation among elderly people: a population-based study. *PLoS One* 2013;8:1-7.
55. Dumurgier J, Elbaz A, Dufouil C, Tavernier B, Tzourio C. Hypertension and lower walking speed in the elderly: the Three-City study. *J Hypertens* 2010;28:1506-14.
56. Gregg EW, Beckles GL, Williamson DF, Leveille SG, Langlois JA, Engelgau MM, et al. Diabetes and physical disability among older U.S. adults. *Diabetes Care* 2000;23:1272-7.
57. Hamer M, Kivimaki M, Lahiri A, Yerramasu A, Deanfield JE, Marmot MG, et al. Walking speed and subclinical atherosclerosis in healthy older adults: the Whitehall II study. *Heart* 2010;96:380-4.
58. Agahi N, Fors S, Fritzell J, Shaw BA. Smoking and physical inactivity as predictors of mobility impairment during late life: exploring differential vulnerability across education level in Sweden. *J Gerontol B Psychol Sci Soc Sci* 2018;73:675-83.
59. Cesari M, Penninx BWJH, Pahor M, Lauretani F, Corsi AM, Rhys Williams G, et al. Inflammatory markers and physical performance in older persons: the InCHIANTI study. *J Gerontol A Biol Sci Med Sci* 2004;59:242-8.
60. Gray VL, Goldberg AP, Rogers MW, Anthony L, Terrin ML, Guralnik JM, et al. Asymptomatic carotid stenosis is associated with mobility and

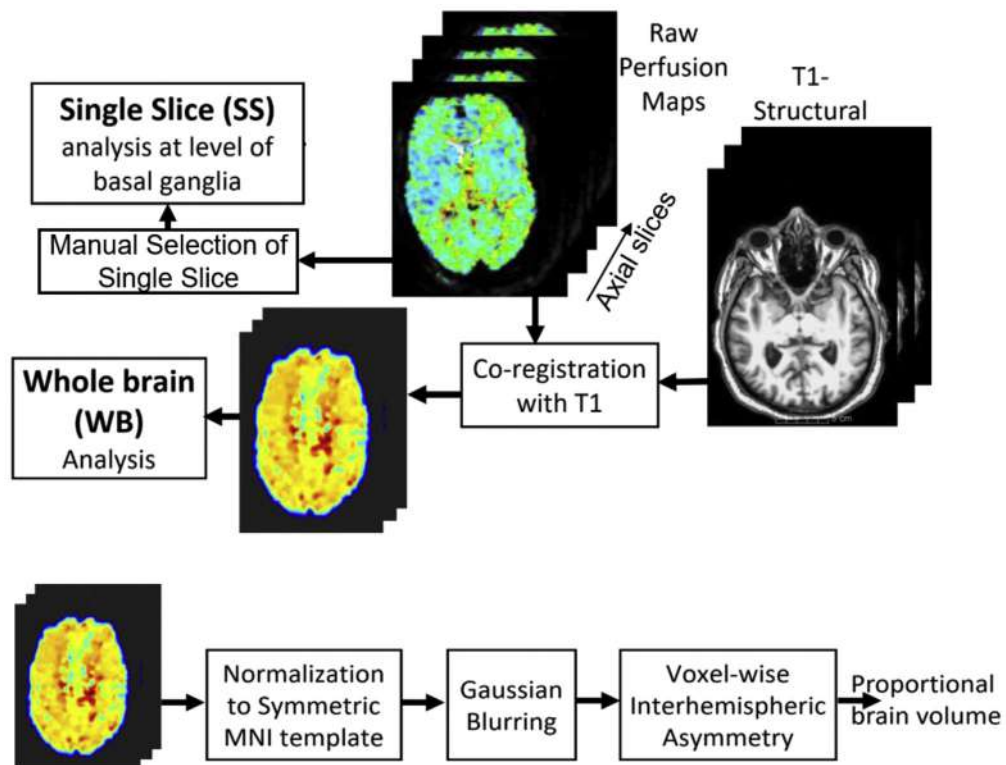
- cognitive dysfunction and heightens falls in older adults. *J Vasc Surg* 2020;71:1930-7.
61. Deweese JA, May AC, Lipchik EO. Anatomic and hemodynamic correlations in carotid artery stenosis. *Stroke* 1970;1:149-57.
  62. Warwick R, Sastry P, Fontaine E, Poullis M. Carotid artery diameter, plaque morphology, and hematocrit, in addition to percentage stenosis, predict reduced cerebral perfusion pressure during cardiopulmonary bypass: a mathematical model. *J Extra Corpor Technol* 2009;41:92-6.
  63. Young DF, Cholvin NR, Roth AC. Pressure drop across artificially induced stenoses in the femoral arteries of dogs. *Circ Res* 1975;36:735-43.
  64. Cebra JR, Putman CM, Pergolesi R, Burgess JE, Yim P. Multi-modality image-based models of carotid artery hemodynamics. *Proc SPIE Med Imaging* 2004;5369:529-38.

Submitted Apr 27, 2020; accepted Oct 3, 2020.

*Additional material for this article may be found online at [www.jvascsurg.org](http://www.jvascsurg.org).*

**CME Credit Available to JVS Readers**

Readers can obtain CME credit by reading a selected article and correctly answering four multiple choice questions on the Journal Web site ([www.jvascsurg.org](http://www.jvascsurg.org)). The CME article is identified in the Table of Contents of each issue. After correctly answering the questions and completing the evaluation, readers will be awarded one *AMA PRA Category 1 Credit*<sup>™</sup>.



**Supplemental Fig (online only).** Overall schematic for computing the interhemispheric perfusion deficit. Single slice (SS) and whole brain (WB) analyses provided asymmetry metrics (left vs right hemispheres) for quantifying and lateralizing perfusion deficits. The proportional brain volume provides an objective measure of the actual regions of the brain with perfusion deficits compared with the whole brain.



**Supplementary Table I (online only).** Patient demographics, vascular risk factors, and stenosis measurements

Characteristic	Mean ± SD or % (No.)
<b>Clinical</b>	
Age, years	67 ± 11
Male sex	85 (17)
White race	55 (11)
Diabetes mellitus	45 (9)
Coronary artery disease	25 (5)
Hypertension	80 (16)
Smoking (past or present)	70 (14)
Hyperlipidemia	55 (11)
<b>Stenosis features</b>	
Minimal diameter at stenosis, mm	1.42 ± 0.4
Minimal area at stenosis, mm <sup>2</sup>	2.32 ± 1.31
MSA	0.65 ± 0.1
MSD	0.83 ± 0.1
Unilateral stenosis	90 (18)
Bilateral stenosis	10 (2)
Left-sided stenosis	50 (10)
PSV at stenosis, ipsilateral side, cm/s	436 ± 141
PSV on contralateral side, cm/s	119 ± 72
Velocity in vertebral arteries, cm/s	
Ipsilateral side	53 ± 18
Contralateral side	57 ± 17
MSA, maximum stenosis by area; MSD, maximum stenosis by diameter; PSV, peak systolic velocity; SD, standard deviation.	

**Supplementary Table II (online only).** Interhemispheric asymmetries for entire cohort

Variable	SS-BG	WB
TTP	0.84 ± 0.63 (0.06-2.16)	0.54 ± 0.33 (0.01-1.22)
MTT	0.63 ± 0.34 (0.17-1.4)	0.46 ± 0.29 (0.05-0.94)
rCBF	4.07 ± 2.75 (0.67-11.61)	2.6 ± 1.4 (0.63-5.5)
rCBV	11.82 ± 13.54 (0.53-42.84)	7.36 ± 7.73 (0.1-29.82)
MTT, mean transit time; rCBF, relative cerebral blood flow; rCBV, relative cerebral blood volume; SS-BG, single-slice at basal ganglia; TTP, time to peak; WB, whole brain. Data presented as mean ± standard deviation (range).		